Discover Oncology

Research

Aberrant expression of CNTRL was associated with poor prognosis, immune response and progression in glioma

Xiaoping Mei[1] · Deyuan Qin[2] · Min Zou[3] · Hongli Teng[4] · Yang Zhai[5]

Received: 12 December 2024 / Accepted: 29 April 2025
Published online: 09 May 2025

Abstract
This study investigated the biological functions and prognostic significance of centromere protein L (CNTRL) in glioma. mRNA expression data and clinical information were obtained from TCGA, CGGA, and an independent cohort of 207 glioma patients. CNTRL expression levels were quantified using qRT-PCR. Functional analyses, including Gene Ontology and KEGG pathway enrichment, were conducted to elucidate the biological roles of CNTRL. Kaplan–Meier survival curves and Cox regression analyses were applied to evaluate its association with overall survival, and a nomogram was constructed to predict individual survival. Additionally, the tumor microenvironment and immune cell infiltration were analyzed. Glioma cell lines were transfected with CNTRL-targeting shRNA to explore its functional role in cell proliferation, migration, and invasion, utilizing CCK-8, colony formation, scratchy and Transwell assays. The results revealed that CNTRL is ubiquitously expressed in brain tissues and is significantly upregulated in glioma. Higher CNTRL expression was positively correlated with increased tumor grade and were associated with poor prognosis in glioma patients. Furthermore, univariate and multivariate Cox regression analyses identified CNTRL as an independent prognostic factor for glioma survival. The nomogram model integrating CNTRL expression and clinical parameters demonstrated robust predictive performance for patient survival. Functional enrichment analyses suggested that CNTRL is involved in key cellular processes such as cell cycle, DNA repair, and chromatin remodeling. CNTRL expression was positively associated with enhanced immune cell infiltration and activation within the tumor microenvironment, as well as with the expression of immune checkpoint molecules, implicating its potential role in immune evasion mechanisms. In vitro, CNTRL knockdown significantly inhibited glioma cell proliferation, migration, and invasion. Notably, suppression of CNTRL led to reduced expression of the cell cycle regulator WEE1 in glioma cells. This study provides comprehensive evidence that CNTRL contributes to glioma progression by regulating the cell cycle and immune-related processes. Targeting CNTRL could represent a promising therapeutic strategy for glioma. These findings underscore the potential of CNTRL as a prognostic biomarker and a therapeutic target in glioma management.

Keywords Glioma · CNTRL · Prognosis · Immune infiltration · Tumor progression

Xiaoping Mei, Deyuan Qin and Min Zou contributed equally to this work.

Supplementary Information The online version contains supplementary material available at https://doi.org/10.1007/s12672-025-02531-1.

✉ Hongli Teng, thl555@163.com; ✉ Yang Zhai, zhaoiy125@163.com | [1]Medical Administration Division, Guangxi International Zhuang Medicine Hospital, Nanning 530200, Guangxi Province, China. [2]Graduate School, Guangxi University of Traditional Chinese Medicine, Nanning 530200, Guangxi Province, China. [3]Department of Pediatrics, Guangxi International Zhuang Medicine Hospital, Nanning 530200, Guangxi Province, China. [4]Pain Management, Guangxi International Zhuang Medicine Hospital, No. 8, Qiuyue Road, Wuxiangxin District, Nanning 530200, Guangxi Province, China. [5]Medical Administration Division, Nanning Seventh People's Hospital, Xingning District, No. 209 Gonghe Road, Nanning 530000, Guangxi Province, China.

1 Introduction

Gliomas are the most common primary tumors of the central nervous system, accounting for approximately81% of intracranial malignancies, and represent a significant threat to human health [1]. These tumors originate from glial cells and encompass diverse histological subtypes including astrocytoma, oligodendrogliomas, ependymomas, and mixed glioblastomas [2]. The 5th edition of the WHO classification emphasize the heterogeneity of gliomas, underscoring the necessity of tailored therapeutic strategies. Despite advancements in surgical techniques, chemotherapy, and immunotherapy, the prognosis for glioma patients remains dismal, with median survival often less than two years [3]. Early diagnosis and aggressive intervention are critical due to the rapid progression of these tumors [4]. The molecular mechanisms underlying glioma genesis are complex and not fully elucidated. Tumor heterogeneity, epigenetic regulation, and the presence of the blood–brain barrier present formidable challenges to the development of effective targeted therapies [5]. Dysregulated expression of oncogenes and tumor suppressor genes has been implicated in glioma initiation and progression, highlighting the urgency of identifying novel therapeutic targets [6]. Furthermore, the discovery of prognostic and predictive biomarkers has facilitated patient stratification and enhanced risk assessment. A comprehensive understanding of glioma biology is essential for the development innovative diagnostic tools and therapeutic approaches.

The Centromere Protein L (CNTRL, also known as CEP110) gene plays a critical role in cell division [7]. The protein encoded by the CNTRL gene is involved in the regulation of cell cycle, particularly during mitosis [8]. It ensures the accurate distribution of chromosomes to daughter cells during cell division, which is essential for maintaining genomic stability [9]. CNTRL, as a centromeric protein is also crucial for centrosome function. The centrosome is an organelle responsible for organizing microtubules, which are part of the cytoskeleton and is vital for proper cell division. It organizes the spindle apparatus to ensure even chromosomes distribution during mitosis [10]. Mutations or dysfunctions in the CNTRL gene are associated with various human diseases. For instance, mutations in CNTRL gene can lead to centrosome dysfunction, which has been linked to certain cancers and developmental abnormalities [11]. Studies have shown that aberrant CNTRL expression can disrupt cell division, contributing to tumorigenesis. Zeng et al. reported CNTRL was highly expressed in hepatocellular carcinoma, and was associated with poor survival outcomes and immune infiltration. Park observed CNTRL/FGFR1 fusion transcript in nasopharyngeal carcinoma, which may be linked to myeloid neoplasms, with Dysregulated signaling pathways in CNTRL-FGFR1-induced myeloid and lymphoid malignancies in both human and mouse models [12–14]. In breast cancer, CNTRL mutation occur in over 5% of cases, and may function as a driver oncogene [15]. Additionally, CNTRL has been implicated in regulating the cell cycle in human esophageal squamous cell carcinoma through ANO9 [16]. These findings highlighted as a potential cancer driver gene. Given the important role of CNTRL in cancer biology, understanding its function is crucial for elucidating disease mechanisms, particularly in cancer. However, the biological functions and prognosis significance of CNTRL in glioma remain unclear. Investigating CNTRL in glioma may provide valuable insights into fundamental questions regarding cell cycle regulation and centrosome function in this malignancy. Overall, the CNTRL gene plays an indispensable role in cell division and is essential for normal cell function and tissue health. In the present study, we comprehensively evaluated the prognostic significance and biological roles of CNTRL in glioma. Our findings contribute to a deeper understanding of glioma, offering insights into risk management, mechanistic pathways, and the development of novel therapeutic strategies.

2 Methods

2.1 Patients and samples

This study utilized two publicly available datasets, alongside an independent cohort from our institution. Gene expression and clinical data for 1018 glioma patients were retrieved from the Chinese Glioma Genome Atlas (CGGA) database, which included information on gender, age, tumor grade, treatment history, IDH mutation status, 1p19q co-deletion status, survival time, and survival status. These data were used as the training set. Transcriptome data for TCGA-GBM (n = 163) and TCGA-LGG (n = 518) were obtained from the Cancer Genome Atlas, log2-transformed and subjected to analysis. Clinical data was also collected for this validation set, excluding samples with incomplete information or survival times less than 30 days. Additionally, expression profiles from 207 healthy controls

were obtained from the GTEx database. Immunohistochemical results of CNTRL and WEE1 were sourced from the Human Protein Atlas (https://www.proteinatlas.org/).

Furthermore, tumor tissue samples and clinical data for glioma patients who underwent surgical treatment at our hospital between 2015 and 2018 were collected. The primary endpoint was death, and patients followed up every three months to record their survival time and status. This cohort served as an independent validation set. This study was approved by the Medical Ethics Committee of Guangxi International Zhuang Medicine Hospital, in accordance with the Declaration of Helsinki. Informed consent was obtained from all participants.

2.2 Bioinformatic analysis

Human brain expression, sub-cellular localization, and immunohistochemical data for CNTRL were obtained from the Human Protein Atlas. Gene alterations were retrieved from cBioPortal, while the protein–protein interaction network was constructed from STRING, with interactions having a score greater > 0.4. Differential expression analysis was performed with the "limma" package in R, and Gene Ontology (GO) and Kyoto Encyclopedia of Genes and Genomes (KEGG) pathway enrichment analyses were carried out on CNTRL-associated genes ($r > 0.6$, $P < 0.001$). Data visualization was achieved with the "ggplot2," package, and statistical analysis was conducted with cluster Profiler, package considering $P < 0.05$ as statistically significant.

Kaplan–Meier survival analysis was performed Using CGGA, TCGA, and our cohort data to compare survival curves between high and low CNTRL expression groups, including stratified analyses by various factors: age (median: age > 41, age < = 41), gender (male, female), histology, primary, recurrent and second, WHO stage (II, III, IV) codeletion status (codel, non-codel), IDH mutant and wildtype, radiotherapy (No, Yes) and chemotherapy (No, Yes). Univariate and multivariate Cox regression analyses were conducted to identify CNTRL as an independent prognostic factor for in glioma patients, with hazard ratios (HRs) and 95% confidence intervals (CIs) calculated. A nomogram risk score model incorporating CNTRL and clinical parameters was developed, with receiver operating characteristic (ROC) curves generated and area under the curves (AUC) calculated. Calibration plots were used to assess the correlation between predicted and actual probabilities at one, three, and five years.

The ESTIMATE algorithm was used to assess stromal and immune scores across CNTRL expression levels in glioma, while immune cell infiltration was evaluated using the CIBERSORT algorithm, which assessed 26 immune cell types. Data visualization was performed using the "Limma" and "ggpubr" packages, with $P < 0.05$ considered statistically significant.

Furthermore, correlations between CNTRL expression and immunotherapy response were assessed using the Tumor Immunotherapy Gene Expression Resources, focusing on TIDE, microsatellite instability (MSI), dysfunction, and exclusion. Small molecular compounds related to CNTRL expression and drug sensitivity were identified using the CellMiner database.

Finally, single-cell transcriptome analysis was conducted using the online tool scCacner Explorer (https://bianlab.cn/scCancerExplorer) [17]. The dataset from the GEO dataset (GSE103224), including 8 samples of high-grade glioma [18], was analyzed to examine CNTRL expression in different cell type, locations, genders as well as its association with cell cycle.

2.3 Cell culture and transfection

The U87 (TCHu138) and U251 (U-251MG) cell lines were obtained from Shanghai Cell Line and Bank (Shanghai, China), while normal human astrocytes HA (ATCC-1087) was sourced from Procell Life Science &Technology (Wuhan, China). Cells were cultured in DMEM medium (Gibco, USA) supplemented with 10% fetal bovine serum (FBS, FS301-02, TRANSGEN, Beijing, China) and 1% penicillin–streptomycin (Gibco, USA) at 37 °C in a humidified incubator with 5% CO_2. To generate CNTRL knockdown cells, shRNA sequences targeting CNTRL were cloned into pMD2G and psPAX2 vectors (GenePharma, Shanghai, China). The resulting sh-CNTRL lentiviruses were used to infect U87 and U251 cells, generating CNTRL knockdown groups. Cells were infected with sh-CNTRL or cDNA-CNTRL lentiviruses when they reached 30–50% confluence. After 48 h of incubation at 37 °C, fresh medium was added, and cells were cultured for an additional 24 h. To select for stably transduced cells 8 µg/ml puromycin (Gibco, USA) was added to culture medium.

2.4 Quantitative real-time PCR

RNA was extracted from the tissue samples using TRIzol reagent (ThermoFisher, USA). and reverse transcribed into cDNA (4368814; Applied Biosystems, Foster City, CA, USA) using the ALL-in-oneTM miRNA First-Strand Reverse Transcription Kit 2.0 (Sangon Biotech, Shanghai, China). Quantitative PCR (qPCR) analysis was performed on the LightCycler480 system (Swiss, Roche) using the 2XColor SYBR Green qPCR Master Mix. GAPDH was used as the housekeeping gene to normalize the expression of CNTRL. The PCR primers for CNTRL were as follows: Forward: 5′-CGAACTTCTCCCGCTCTACC-3′; Reverse: 5′-TTTCGTCAGGCACGGTATGT-3′; For WEE1 Forward: 5′-GCTTCCCTCACAGTGGTATG 3′; Reverse: CCGAGGTAATCTACCCTG TCTGA. The PCR primers for GAPDH were as follows: Forward: 5′-GAAGGTGAAGGTCGGAGT-3′; Reverse: 5′-GAAGATGGT GATGGGATTTC-3′.

2.5 Western blot

Tumor cell pellets from each group were lysed with RIPA lysis buffer on ice for 30 min. After centrifugation at 12,000 rpm for 20 min at 4 °C, the supernatant was collected and protein concentration was determined using a protein assay kit. Protein samples were denatured by heating at 100 °C for 10 min. Samples were then separated on a (40–120) g/L SDS-PAGE gel and transferred to a PVDF membrane (ThermoFisher, T2234, USA). The membrane was blocked with 5% skim milk for 1 h at room temperature, followed by overnight incubation with the primary antibody against CNTRL, WEE1 and anti-β-actin (Invitrogen, PA5-54219, USA) overnight at 4 °C. After washing, the membrane was incubated with an HRP-conjugated secondary antibody for 1 h at room temperature. Protein bands were detected using a chemiluminescence detection system.

2.6 CCK-8

The Cell Counting Kit-8 (Beyotime, China) assay was employed to assess the viability of U87 and U251 glioma cells. U87 and U251 cells were seeded in 96-well plates at a density of 10^4 cells per well. After 24 h, 10 µl of CCK-8 solution was added to each well, and cells were incubated for an additional 2 h. Absorbance was measured at 450 nm at 24, 48, 72, 96, and 120 h. For drug sensitivity analysis, various concentrations of Cherlerythrine (0, 5, 10, 15, 20, 25, 30, 35, 40, uM) were added into the control group (U87 and U251 cells) and CNTRL knockdown groups. The cell viability was calculated as: cell viability, $\% = OD_{drug} - OD_{control})/(OD_{control} - OD_{blank})*100\%$.

2.7 Colony formation

A cell counting assay was performed using U87, U251, or sh-CNTRL cells. Cells (200/well) were seeded in 6-well plates and incubated until colonies were macroscopically visible. Subsequently, cells were washed with PBS (2x), fixed with 75% ethanol for 30 min, and stained with 0.4% crystal violet for 15 min. Finally, stained cells (Beyotime, China) were imaged, and the number of cells was counted.

2.8 Scratch assay

For scratchy assay, 5×10^5 cells were seeded into 6-well plates and allowed to proliferate until reaching 90% confluence. A sterile pipette tip was used to create a scratch in the cell monolayer, which was then washed with PBS to remove detached cells. The remaining cells were cultured in a medium containing 2% FBS and incubated at 37 °C in a 5% CO_2 environment. After 36 h, random fields were imaged under a light microscope (Leica, Wetzlar, Germany) for analysis.

2.9 Transwell assay

Well-grown glioma cells were initially starved in serum-free medium. Matrix glue was diluted to 1 mg/ml in serum-free medium on ice and mixed with a pre-cooled suction head. Sixty microliters of the glue were added to the Transwell chamber (Corning, USA) to form a uniform layer, incubated at 37 °C and 5% CO_2 for 3 h, then unbound glue was discarded. One hundred microliters of serum-free culture solution were added, and the plate was incubated at 37 °C for 30 min for

hydration. One hundred thousand cells were added to each chamber and cultured with 200 µl serum-free medium. Six hundred microliters of complete medium with 10% fetal bovine serum were added to the 24-well plate, which was then incubated at 37 °C and 5% CO_2 for 24 h. The Transwell chamber was removed, and the medium was discarded; the internal matrix glue and cells were wiped away with a PBS-soaked cotton swab. The chamber was fixed with 4% paraformaldehyde for 30 min, washed with PBS (Gibco, USA), and stained with crystal violet (Beyotime, China) for 20 min. After washing three times with PBS and air drying, the cells were observed under a microscope and counted.

2.10 Statistical analysis

All bioinformatic analyses were performed using R software (Version 4.2.1). Experiments data and visualization were carried out using Graphpad Prism 9 software. Data are expressed using mean ± standard deviation. The student's *t* test was used for comparisons between two groups with assumption of normality, while one-way ANOVA was used for comparisons involving more than two groups followed by Bonferroni's post-hoc test fro multiple comparisons. A $P < 0.05$ was considered statistically significant unless otherwise specified.

3 Results

3.1 CNTRL expression, subcellular localization, gene alterations in brain tissue

HAP data revealed that CNTRL was ubiquitously expressed across all brain regions with low region specificity (Fig. 1A). Analysis identified 44 single cell clusters expressing CNTRL (Fig. 1B). Subcellular localization studies showed CNTRL was present in cytoskeleton, cytosol, nucleus, and plasma membrane (Fig. 1C). In glioma, the gene alteration frequency was below 2% (Fig. 1D), and the copy-number alterations were associated with changes in CNTRL mRNA expression (Fig. 1E). A protein–protein interaction network was constructed, indicating that CNTRL interacts closely with FGFR1, FGFR1OP, PLK1, CEP170, CCDC120, CCDC68, CEP128, ODF2, NIN, and TUBE1 (Fig. 1F).

3.2 CNTRL expression in glioma and its correlation with clinical characteristics

Data from TCGA and GTEx showed significantly elevated CNTRL expression in glioma tissues (Fig. 2A), consistent with results from immunohistochemical staining (Fig. 2B). Further analyses indicated no significant correlation CNTRL expression with clinical age (Fig. 2C), and gender (Fig. 2D). However, expression increased with tumor grade (Fig. 2E), and was higher in GBM than LGG (Fig. 2F). No differences were observed across glioma subtypes (Fig. 2G). Additionally, IDH wildtype and 1p19q non-codeletion glioma exhibited higher CNTRL expression (Fig. 2H, I). Radiotherapy did not affect CNTRL expression (Fig. 2J), but patients receiving chemotherapy showed increased levels (Fig. 2K).

3.3 Independent prognosis analysis and risk scoring system development

Kaplan–Meier survival analysis demonstrated that high CNTRL expression was associated with poorer overall survival (OS) in the CGGA dataset (Fig. 3A), a finding validated in TCGA and an independent cohort (Fig. 3B, C). Univariate cox regression indicated that high CNTRL expression increased mortality risk (CGGA, HR: 2.187, 95% CI 1.898–2.520, $P < 0.001$, Fig. 3D; TCGA: HR: 1.145, 95% CI 1.036–1.266, $P = 0.008$, Fig. 3E; Independent cohort, HR: 1.623, 95% CI 1.248–2.111, $P < 0.001$, Fig. 3F). Multivariate cox regression confirmed that CNTRL was an independent prognostic factor f (CGGA, HR: 1.820, 95%CI: 1.556–2.127, $P < 0.001$, Fig. 3G; TCGA: HR: 1.155, 95% CI 1.038–1.285, $P = 0.008$, Fig. 3H; Independent cohort, HR: 1.467, 95% CI 1.098–1.960, $P = 0.010$, Fig. 3I). A nomogram incorporating CNTRL expression and clinical parameters was constructed to predict individual risk scores (Fig. 3J). The time-independent ROC curves demonstrated predictive accuracy, with AUC values of 0.635 at one year, 0.685 at three years, and 0.722 at five years (Fig. 3K). Calibration plots confirmed the concordance of predicted and observed OS at these time points (Fig. 3L–N). Stratified analyses further indicated that high CNTRL expression correlated with poor OS across various clinical subgroups (age, gender, grade, primary, secondary, recurrent, WHO stage, l19q codeletion status, IDH mutant status, radiotherapy and chemotherapy status) (Fig. 4A–T).

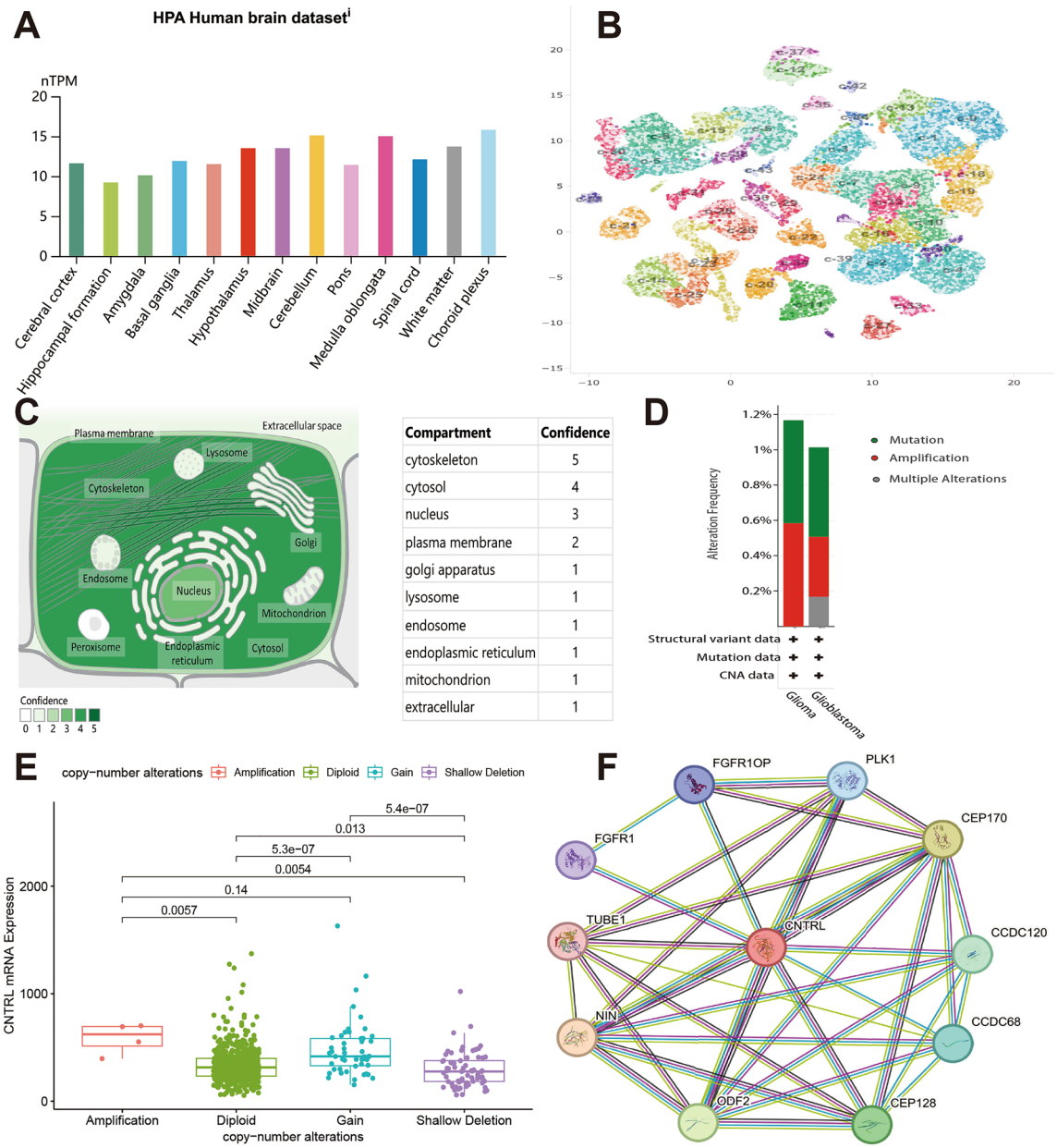

Fig. 1 General characteristics of CNTRL. **A** Region expression of CNTRL in human brain tissues. **B** Single-cell proteome analysis in brain tissue. **C** Subcellular location of CNTRL. **D** Frequency of CNTRL gene alterations in glioma. **E** Correlation between copy umber alterations and CNTRL mRNA expression. **F** Protein–protein interaction associated with CNTRL

3.4 Functional and pathway enrichment analysis

GO enrichment analysis revealed that that CNTRL was primarily associated with chromosome segregation, DNA replication and RNA splicing, nuclear division, ATP hydrolysis activity, histone biding and modifying activity, methylated histone binding, helicase activity, and DNA binding (Fig. 5A). KEGG pathway enrichment highlighted significant roles in the cell cycle, spliceosome, ATP-dependent chromatin remodeling, nucleocytoplasmic transport, ubiquitin mediated proteolysis, polycomb repressive complex, Fanconi anemia pathway, nucleotide excision repair, DNA replication, and homologous recombination (Fig. 5B).

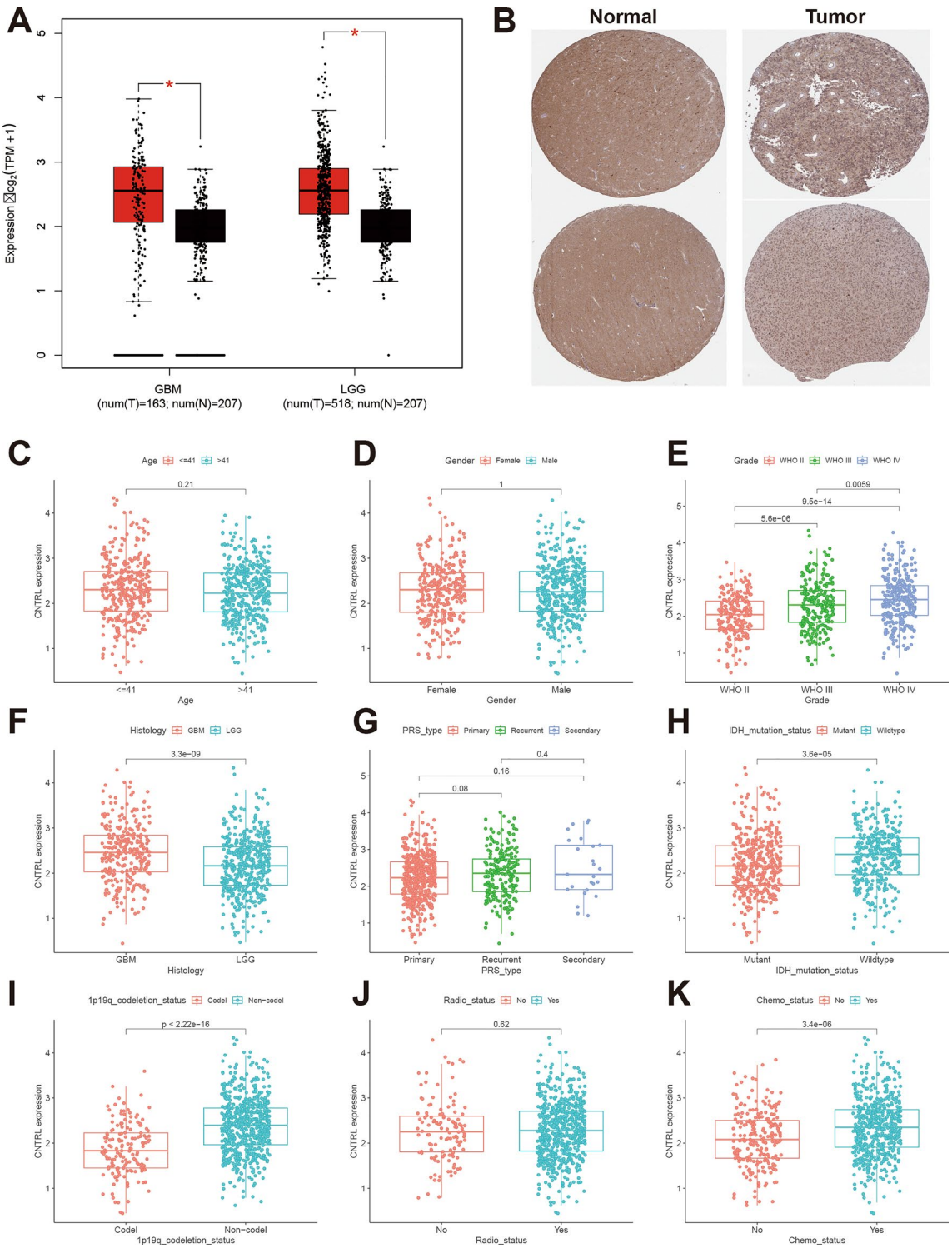

Fig. 2 Abnormal expression of CNTRL in glioma and its correlation with clinical parameters. **A** CNTRL expression levels in GBM, LGG and normal tissue. **B** Immunohistochemistry analysis of CNTRL in glioma and normal tissues. **C–K** CNTRL expression levels stratified by age, gender, tumor grade, histological subtype, PRS type, IDH mutation status, 1p19q codeletion status, radiotherapy and chemotherapy status

3.5 Tumor microenvironment and immune infiltration

The CNTRL high expression group exhibited elevated stromal immune and ESTIMATE scores (Fig. 6A–C). Immune

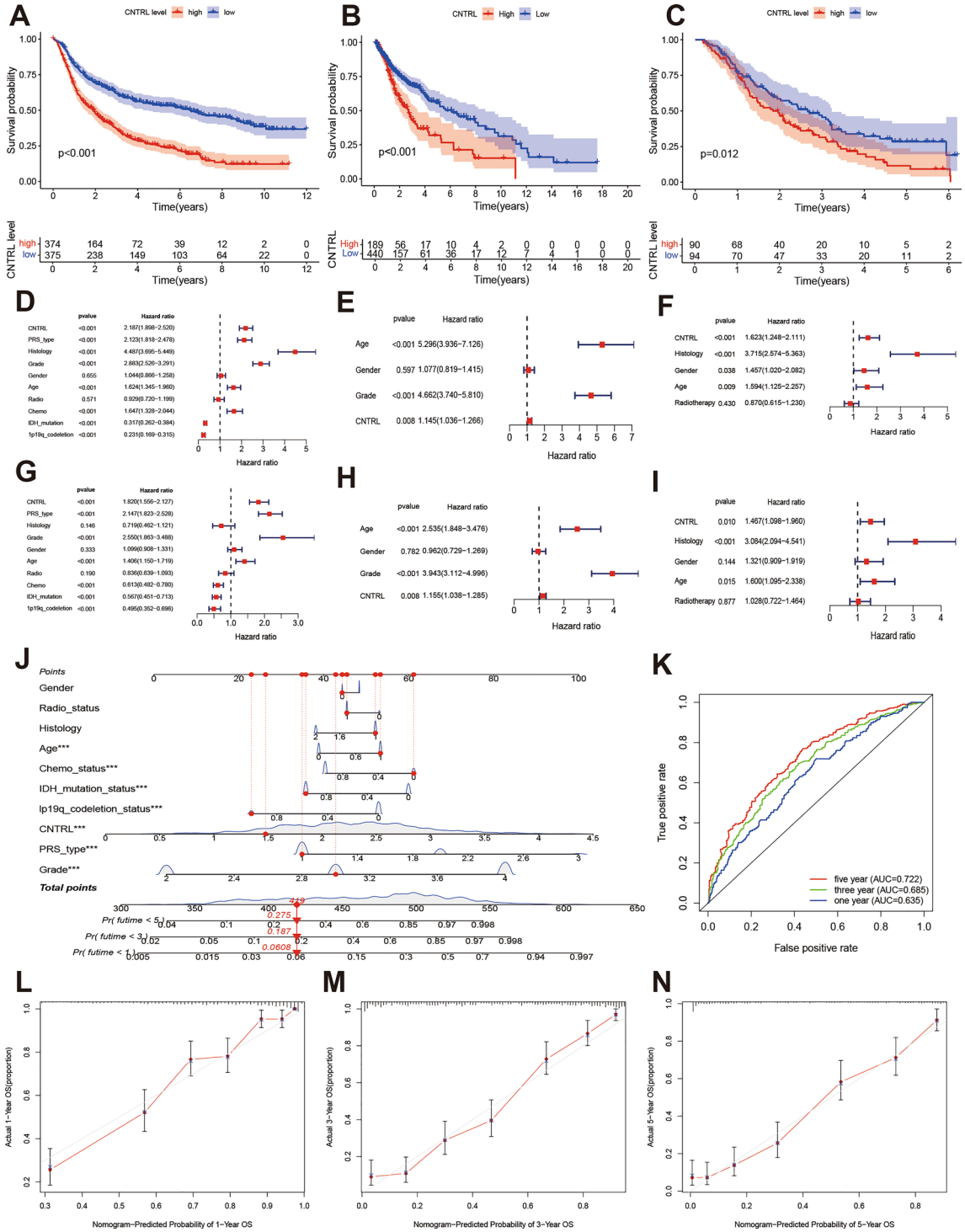

Fig. 3 CNTRL as an independent prognostic predictor in glioma. **A–C** Kaplan-Meire survival curves comparing high and low CNTRL expression groups in the CGGA, TCGA and an independent cohort. **D–F** Univariate cox regression analysis of the correlation of CNTRL expression and prognosis in the CGGA, TCGA, and an independent cohort. **G–I** Multivariate cox regression analysis of correlation between CNTRL expression and prognosis in the CGGA, TCGA, and an independent cohort. **J** Nomogram plot integrating CNTRL expression with clinical parameters. **K** Receiver operating characteristic curves for predicting 1-year, 3-year, and 5-year survival based on CNTRL expression. **L–N** Calibration plots for the nomogram-predicted probabilities of 1-year, 3-year and 5-year overall survival (OS)

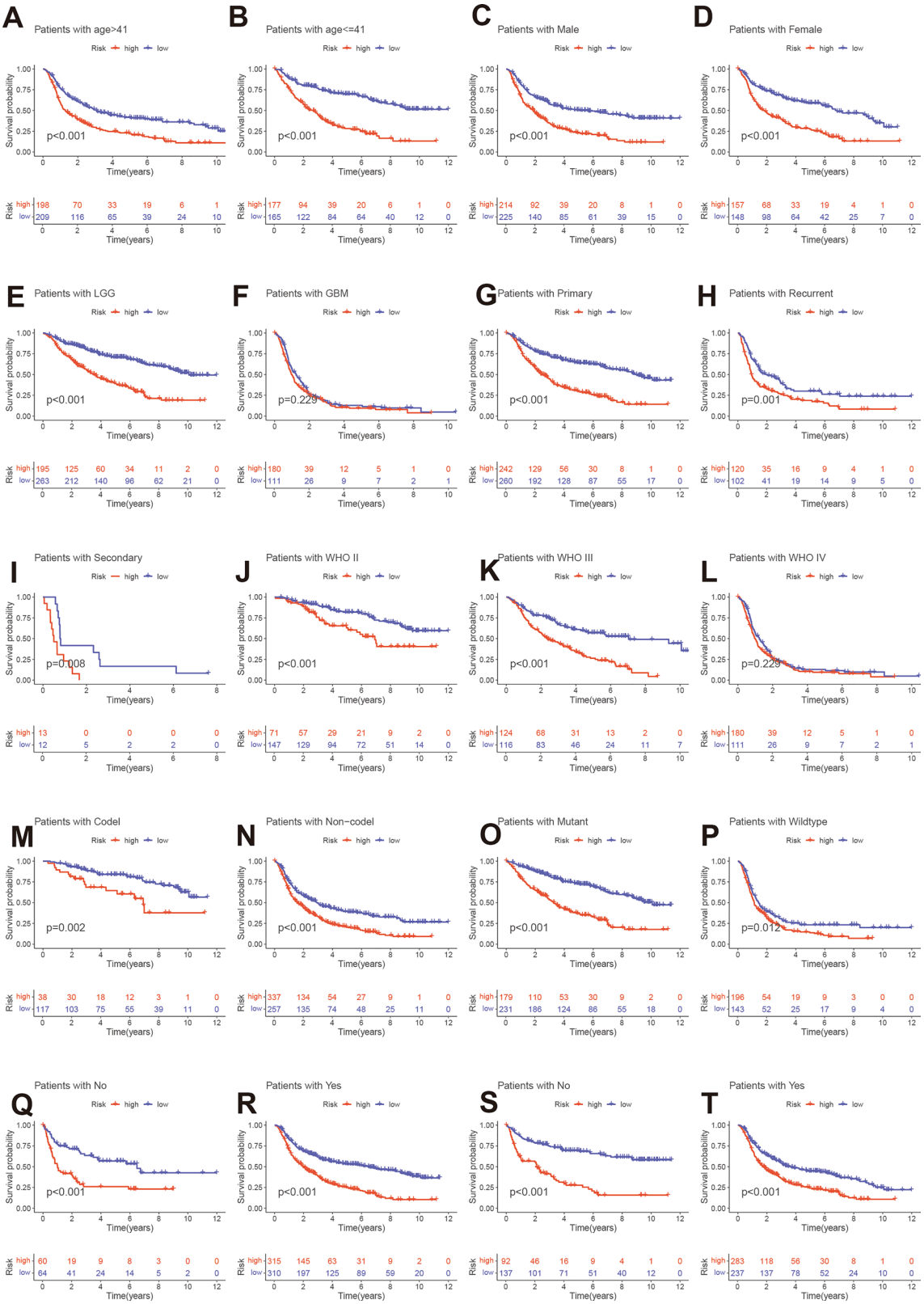

Fig. 4 Stratified analysis of the correlation between CNTRL expression and prognosis in glioma. **A, B** Age > 41 and age ≤ 41 years. **C, D** Male and female. **E, F** LGG and GBM. **G–I** Primary, recurrent and secondary. **K, L** WHO III and WHO IV. **M, N:** 1p19 codeletion and non-codeletion. **O, P** IDH mutant and wildtype. **Q, R** Radiotherapy (NO and Yes). **S, T** Chemotherapy (No and Yes)

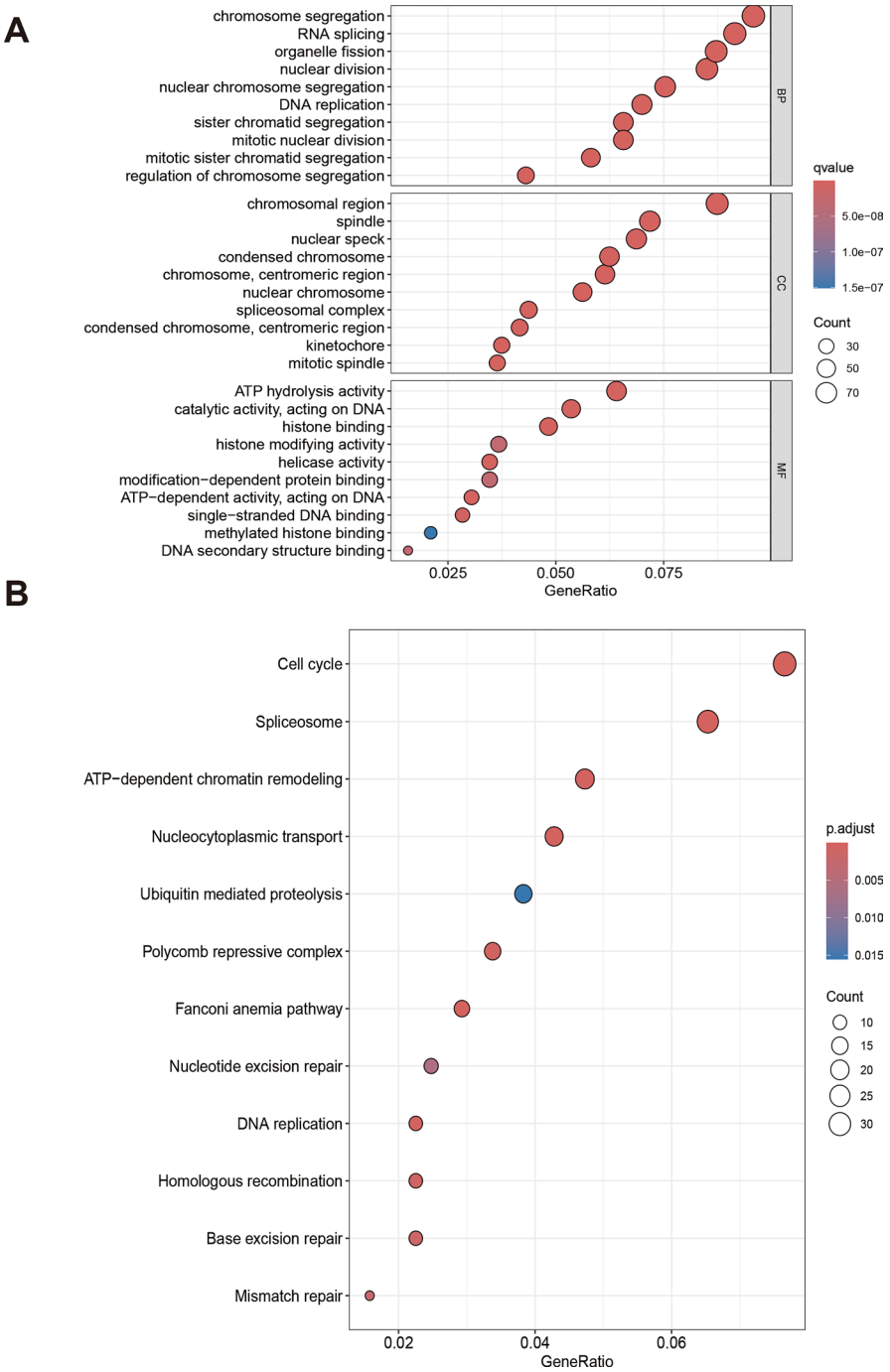

Fig. 5 Function and pathways enrichment analysis of CNTRL. **A** GO function enrichment analysis. **B** KEGG pathway enrichment analysis

infiltration analysis showed increased levels of various immune cells including adCs, B cells, CD8 + T cells, DCs, iDCs, macrophages, mast cells, neutrophils, NK cells, pDCs, T helper cells, Th1 and Th2 cells, TIL and Treg levels (Fig. 6D). Moreover, immune-related processes such as APC co_inhibition/stimulation, CCR, check-point, cytolytic activity, HLA, inflammation-promoting, MHC class I, proinflammation, T cell co_inhibition and stimulation, Type I and II IFN response were significantly enhanced in the CNTRL high-expression group (Fig. 6E). Key immune checkpoint genes were also upregulated such as CD274, PDCD1, VTCN1, LAG3, CD276, CTLA4, ADORA2A, and LGALS9 (Fig. 6F).

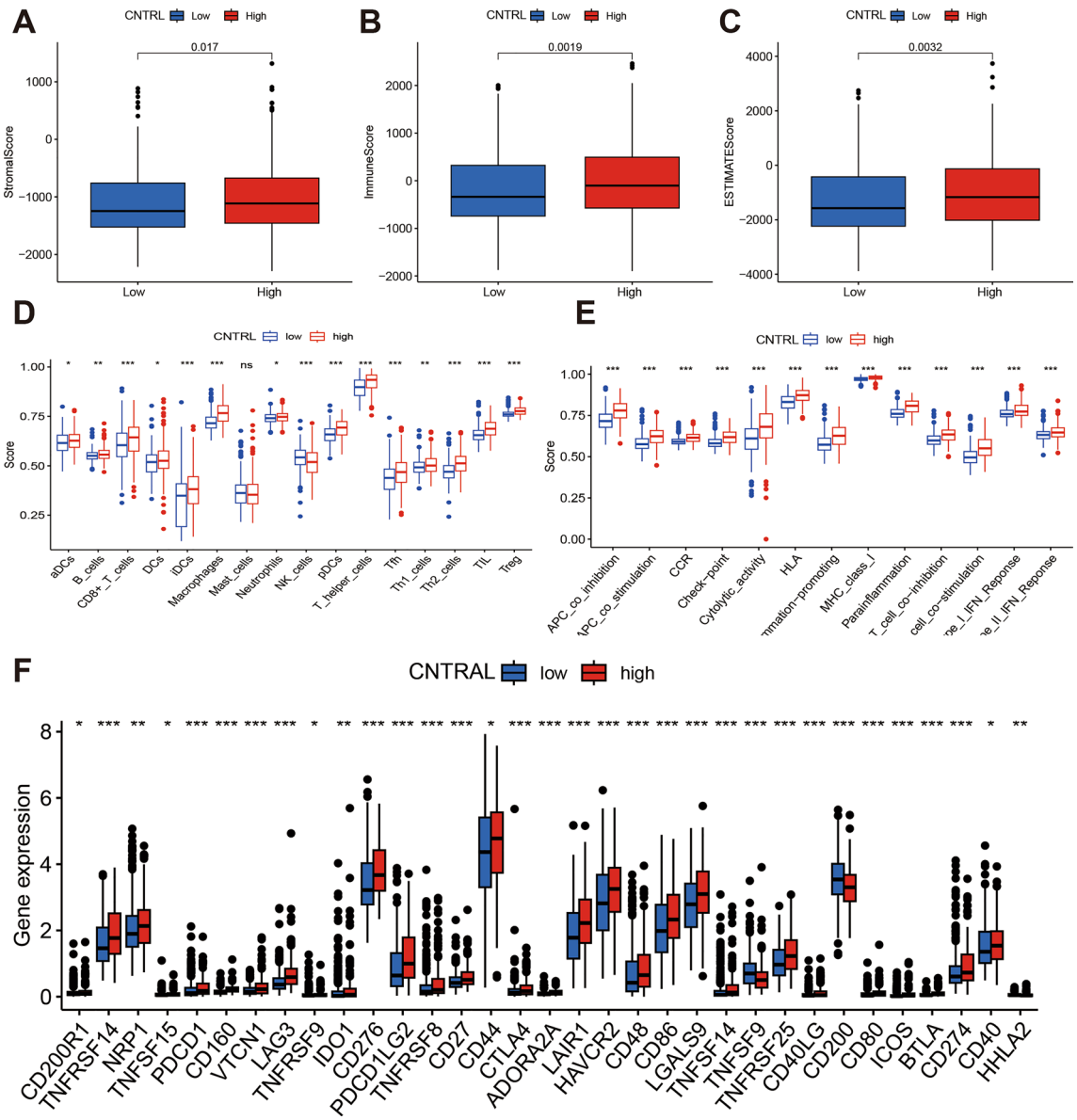

Fig. 6 Tumor microenvironment and immune infiltration levels. **A–C** Comparison of stromal, immune and ESTIMATE scores between high and low CNTRL expression groups. **D, E** Immune cells infiltration levels and immune function i between high and low CNTRL expression groups. **F** The differential expression of immune checkpoint genes between high and low CNTRL expression groups

The correlation analysis indicated that CENTRL expression was positively associated with APC_co_stimulation, B cells, cytolytic activity, HLA, iDCs, MHC class I, para inflammation, T cell co_inhibition, Type II IFN response, Treg, Th2 cells, T helper cells (Fig. 7A–L), while negative associations were found between CNTRL and pDCs, mast cells, Tfh, Th1 cells (Fig. 7M–P).

3.6 Immunotherapy response and drug sensitivity

To evaluate the effect of CNTRL expression on immunotherapy response, we compared some parameters associated with immunotherapy, and found the TIDE, MSI and Dysfunction levels were significantly elevated in CNTRL high expression group,

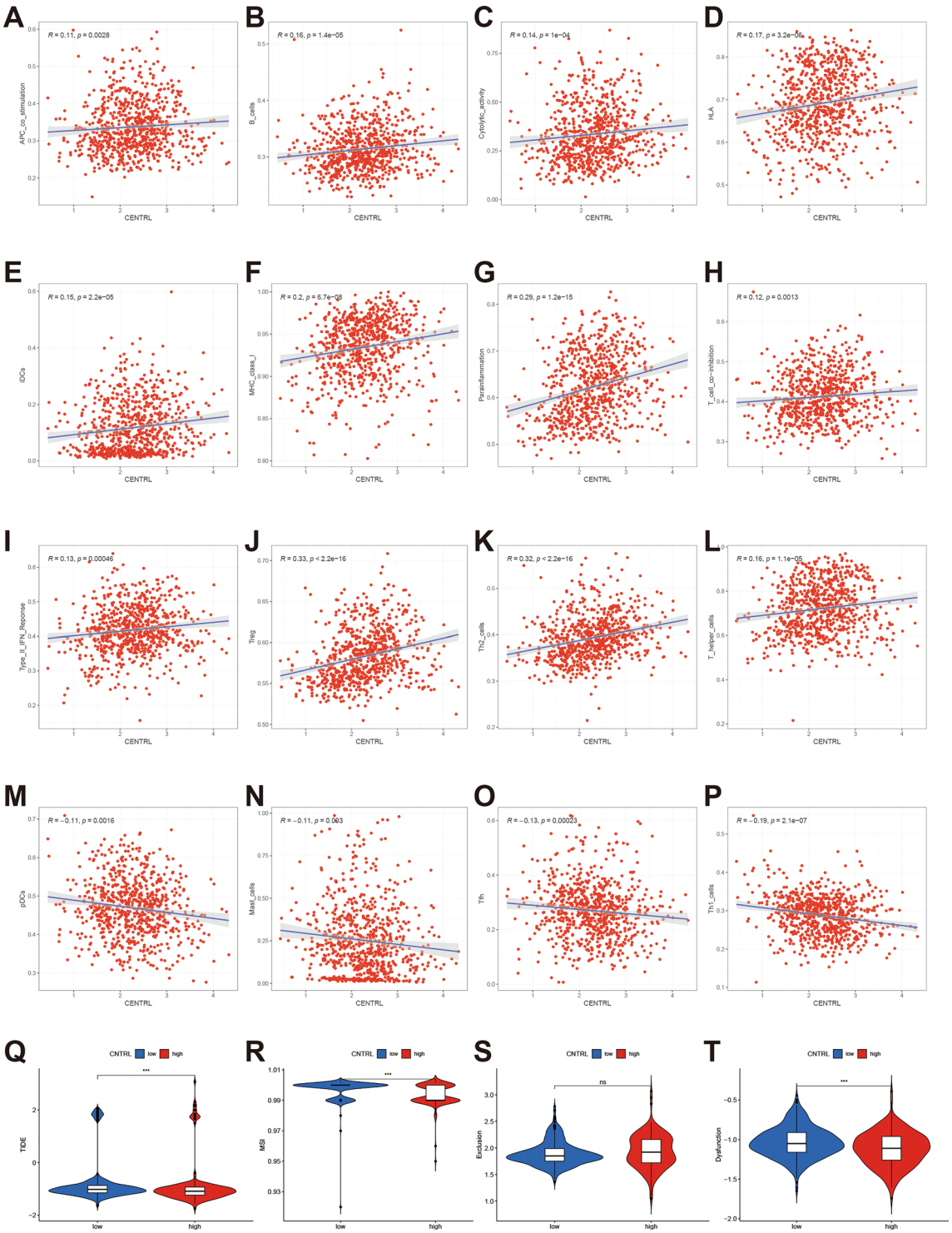

Fig. 7 Correlations of CNTRL expression with immune cells and immunotherapy response. **A** APC co_stimulation, **B** B cells. **C** Cytolytic activity. **D** HLA. **E** iDCs. **F** MHC class I. **G** Para inflammation. **H** T cell co_inhibition. **I** Type II IFN response. **J** Treg. **K** Th2 cells. **L** T helper cells. **M** pDCs. **N** Mast cells. **O** Tfh. **P** Th1 cells. **Q–T** TIDE, MSI, exclusion, and dysfunction between high and low CNTRL expression groups

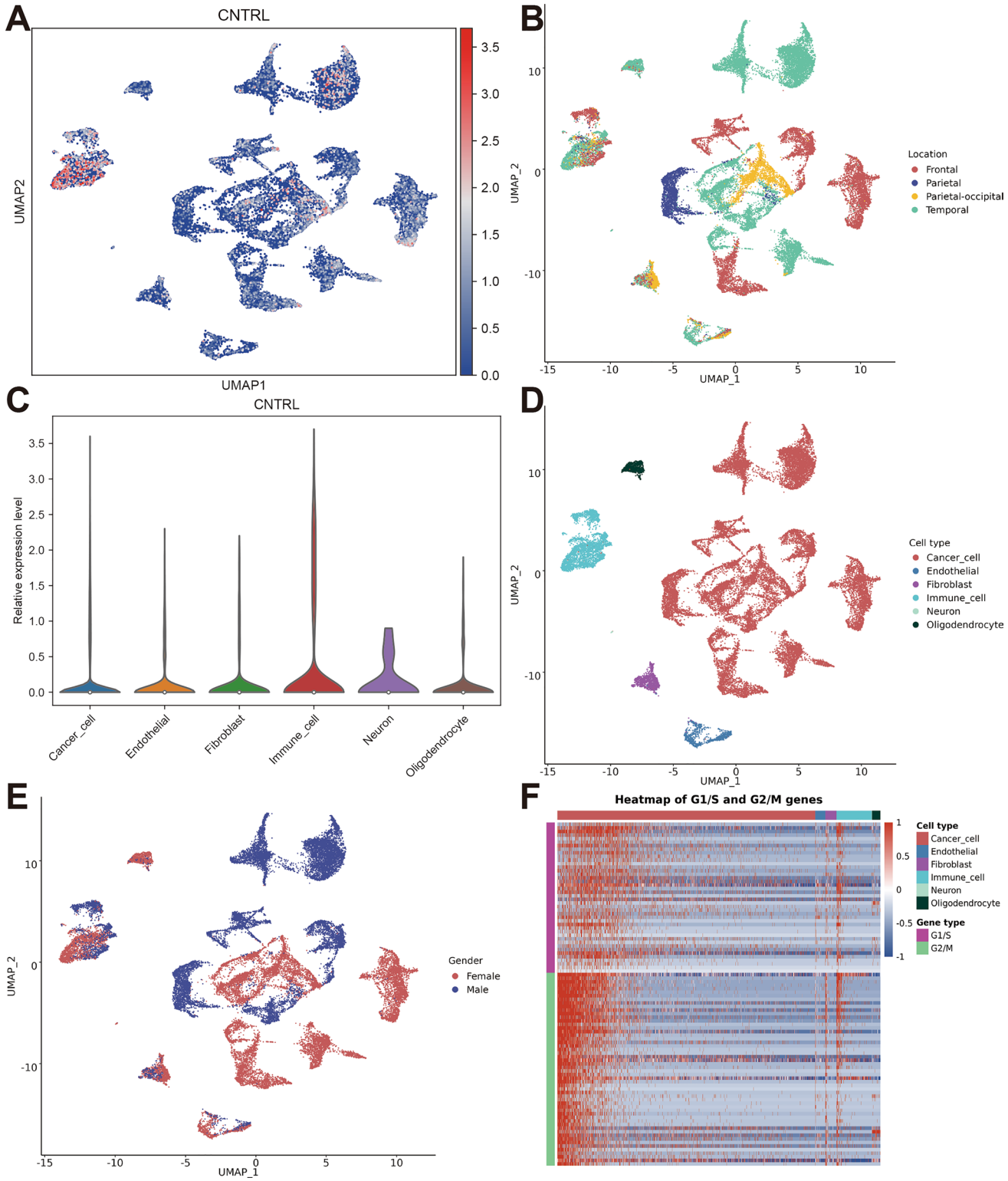

Fig. 8 Single-cell transcriptome analysis of CNTRL in glioma. **A, B** Spatial distribution of CNTRL in glioma. **C, D** Distribution of CNTRL among different cell types. **E** Gender distribution of CNTRL expression. **F** CNTRL distribution across cell cycle

while the exclusion level were significantly decreased in CNTRL high expression group (Fig. 7Q–T). The drug sensitivity analysis indicated that CNTRL expression was positively correlated with sensitivity to multiple small-molecule compounds, particularly Chelerythrine, Nelarabine, Fenretinide, PX-316, Demethylaminopa (Figure S1 8A–P).

Fig. 9 CNTRL promotes glioma cell progression. **A** CNTRL Expression in glioma. **B** CNTRL silencing in glioma cell lines. **C** Western blot validation of CNTRL silencing. **D, E** CCK-8 of U87 and U251 cell growth following CNTRL silencing. **F, G** Colony formation showing inhibition in U87 and U251 cells after CNTRL silencing. **H, I** Migration ability of U87 and U251 cells after CNTRL silencing. **J, K** Invasion ability of U87 and U251 cells after CNTRL silencing. **L, M** Scratch assay results for U87 and U251 cells after CNTRL silencing. *:$P < 0.05$, **:$P < 0.01$, ***:$P < 0.001$; ****:$P < 0.0001$

3.7 Single-cell transcriptome analyses

Single-cell transcriptome analyses revealed that CNTRL were highly expressed in frontal, temporal and parietal-occipital section (Fig. 8A, B), predominantly in cancer and immune cells, with no significant differences among endothelial, fibroblast, neuron and oligodendrocyte (Fig. 8C, D. Notably, CNTRL was enriched in the cell G2/M cell cycle phase and highly expressed in females' temporal and frontal regions (Fig. 8E, F).

3.8 Experiments validation of CNTRL function in glioma cells

Experiments validation confirmed high CNTRK expression in glioma cell lines (Fig. 9A). Knockout of CNTRL (Fig. 9B, C) were built. CCK-8 assay indicated that glioma cells growth was inhibited after knocking out CNTRL (Fig. 9D, E). The number of colony format was significantly decreased in CNTRL knock-out group than control group (Fig. 9F–H). Transwell assay also suggested that the migration and invasion ability of glioma cells was suppressed after CNTRL knock out (Fig. 9I–L). Scratch assay showed similar results (Fig. 9M, N). KEGG pathways analyses indicated that cell cycle pathways were highly enriched in CNTRL high expression (Fig. 10A). The WEE1 gene is one of top 10 enriched genes. A previous study reported that Inhibition of WEE1 in GBM eliminates G2/M block, promotes early entry into mitosis and leads to cell death through mitotic mutation and apoptosis [19]. We validated the WEE1 gene associated with cell Cyle. We also found CNTRL was positively associated with WEE1 expression in glioma (Fig. 10B). The WEE1 was highly expressed in glioma (Fig. 10C). The WEE1 was higher in the CNTRL-high group than that in the CNTRL-low group (Fig. 10D), and the co-expression of CNTRL and WEE1 have poor prognosis that other groups (Fig. 10E). The Western blot showed the WEE1 was down-regulated in CNTRL knock-out groups (Fig. 10F). Furthermore, the WEE1 protein and RNA expression levels were inhibited after knock outing CNTRL in glioma cells (Fig. 10G, H). Finally, we found Cheleyrthrine suppressed the cell viability more markedly in the CNTRL knockout group (Fig. 10I, J). The CNTRL may involve in glioma progression via regulating cell cycle.

4 Discussion

This study presents several significant findings: (1) CNTRL is identified as a highly expressed gene in glioma, with its expression levels positively correlated with tumor grade and poor prognosis. Univariate and multivariate Cox regression analyses confirmed CNTRL as an independent prognostic factor for glioma survival. A nomogram incorporating CNTRL and clinical parameters demonstrated reliable predictive performance for patient survival. (2) Functional enrichment analysis revealed that CNTRL contributes to glioma progression by regulating critical biological processes such as cell cycle, DNA repair, and chromatin remodeling CNTRL expression is also associated with immune cell infiltration, immune activation, and immune checkpoint molecules, suggesting its involvement in immune escape mechanisms. (3) CNTRL is a potential therapeutic target; Knockdown of CNTRL in glioma cell lines significantly inhibited cell proliferation, migration, and invasion, highlighting its potential as a therapeutic target. Through integrated analysis of multiple databases, this study demonstrated that CNTRL is abnormally expressed in glioma and serves as an independent prognostic biomarker. These findings were validated in two independent cohort datasets. Additionally, the study constructed a nomogram-based risk prediction model combining CNTRL expression and clinical parameters, reinforcing its prognostic significance in glioma.

The CNTRL protein, a key i centrosome component, play essential roles in centrosome maturation and microtubule organization [9]. Previous studies have linked CNTRL to various cancers. Zeng et al. demonstrated high CNTRL expression in hepatocellular carcinoma, correlating with poor patient outcomes and altered immune infiltration

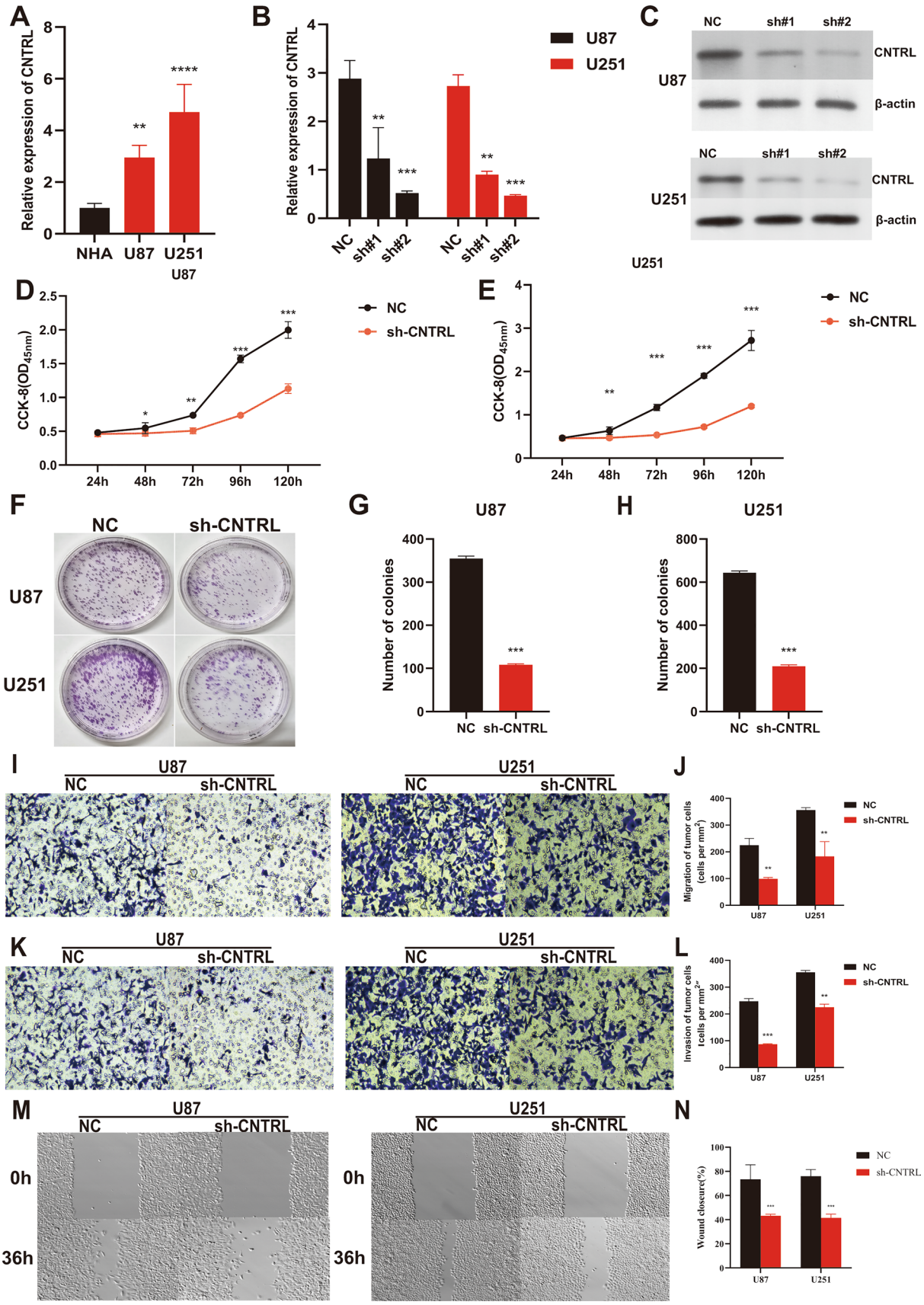
A
Relative expression of CNTRL
NHA U87 U251
B
Relative expression of CNTRL
U87
U251
NC sh#1 sh#2
C
NC sh#1 sh#2
U87
CNTRL
β-actin
U251
D
CCK-8(OD45nm)
NC
sh-CNTRL
24h 48h 72h 96h 120h
E
CCK-8(OD45nm)
F
NC sh-CNTRL
U87
U251
G
U87
Number of colonies
NC sh-CNTRL
H
U251
I
U87
U251
NC sh-CNTRL
J
Migration of tumor cells (cells per mm2)
K
Invasion of tumor cells (cells per mm2)
L
M
0h
36h
N
Wound closure(%)

Fig. 10 CNTRL regulated WEE1 expression level and drug sensitivity analyses. **A** Cell cycle pathways enriched in high CNTRL expression group. **B** Correlation scatterplot between CNTRL and WEE1 expression in glioma. **C** Immunohistochemistry of WEE1 in glioma and normal tissue. **D** Kaplan-Meire curves of glioma patients stratified by CNTRL and WEE1 co-expression. **E** Western blot showing protein expression in U87 and U251 cells following CNTRL silencing. **F** Protein expression levels of WEE1 in U 87 and U251 cells with CNTRL silencing. **G, H** RNA expression levels of WEE1 in U87 and U251 cells with CNTRL silencing. **I, J** Effect of Chelerythrine on cell viability in U87 and U251 with CNTRL silencing. *:$P < 0.05$, **:$P < 0.01$, ***:$P < 0.001$; ****:$P < 0.0001$

[12]. Park et al. reported the presence of a CNTRL/FGFR1 fusion transcript in nasopharyngeal carcinoma, potentially linked to myeloid neoplasms. Dysregulated signaling pathways involving FGFR1 have been observed in CNTRL-FGFR1-induced malignancies in both human and mouse models [13]. Previous studies reported that CNTRL-FGFR1 fusion oncogene contributes to the development of dominant leukemias by aberrantly activating several signaling pathways involved in the development and differentiation of myeloid and T lymphocytes [14, 20]. In breast cancer, CNTRL mutations exceed 5% and are considered potential oncogenic drivers [15]. Furthermore, CNTRL has been implicated in cell cycle regulation in human esophageal squamous cell carcinoma, specifically in the context of ANO9 signaling [16]. These findings collectively underscore the critical role of CNTRL as a cancer driver gene. However, the role and function of CNTRL in glioma have been rarely reported.

Our functional experiments confirmed that CNTRL plays a pivotal role in glioma progression. CNTRL was highly expressed in glioma cell lines, and its knockdown inhibited cell proliferation, colony formation, migration, and invasion. We also investigated the relationship between CNTRL and FGFR1 and found a weak correlation. This suggests that CNTRL may exert its biological function through alterative mechanisms in glioma. Using a correlation coefficient greater than 0.6 and $P < 0.001$, we identified several co-expression genes associated with CNTRL. GO function and KEGG pathway enrichment analyses were performed. We found CNTRL were primarily enriched in nucleotide binding and mitotic, including chromosome segregation, RNA splicing, DNA replication, and mitotic sister chromatid segregation. The main pathway enriched for CNTRL was the cell cycle, followed by spliceosome, ATP-dependent chromatin remodeling, nucleocytoplasmic transport, and ubiquitin mediated proteolysis. Disruptions in the tightly regulated cell cycle often led to uncontrolled cell division and proliferation, a hallmark of tumorigenesis [21, 22]. WEE1, one of the top 10 enriched genes, was of particular interest. A previous study reported that Inhibition of WEE1 in GBM eliminates G2/M block, promotes early entry into mitosis and leads to cell death through mitotic mutation and apoptosis [19]. Preliminary experiments indicated that CNTRL inhibition significantly reduced WEE1 expression in glioma cells. Aberrant tumor cell proliferation, commonly observed in the early stages of cancer, is often linked to dysregulation of cell differentiation, cell cycle activity, mitosis. Dysregulation of the cell cycle has become a key feature of most cancers, frequently due to mutations in genes that regulate cell cycle control [23, 24]. Gliomas are no exception, and cell cycle dysregulation is closely associated with the occurrence and development of glioma [25].

The tumor microenvironment (TME) and immune infiltration play pivotal roles in glioima initiation and progression. The TME consists of tumor cells, immune cells, endothelial cells, extracellular matrix, and other components, characterized by significant hypoxia, metabolic reprogramming, and immunosuppressive properties [26]. Gliomas suppress effective immune responses by secreting immunosuppressive factors such as TGF-β and IL-10 and recruiting regulatory T cells (Tregs) and myeloid-derived suppressor cells (MDSCs) [27]. Additionally, tumor-associated macrophages (TAMs) undergo a shift from the M1 to the M2 phenotype, further promoting tumor cell proliferation, invasion, and immune evasion [28]. Previous studies have confirmed the relationship between immune regulation and glioma progression [29]. Research focused on immune modulation could provide new therapeutic strategies for gliomas. Immune checkpoint inhibitors, the most extensively studied and used immunotherapies, have demonstrated significant anti-tumor effects in various cancers [30]. Other immunotherapies such as CAR-T cell therapy, cytokine therapy, oncolytic viral therapy, and tumor vaccines have also been FDA-approved; however, their application in gliomas faces significant challenges. The blood–brain barrier, a unique structure in the central nervous system, restricts the entry of most anti-tumor drugs and cells into the brain. Additionally, gliomas have an immunosuppressive microenvironment characterized by high levels of immune inhibitory molecules, such as PD-L1 and IDO, as well as an abundance of immunosuppressive cells like tumor-associated macrophages and regulatory T cells [31]. Furthermore, the low mutational burden of gliomas limits the number of therapeutic targets available to the immune system. These immune characteristics have hindered the efficacy of immunotherapy in glioma treatment [32–34]. Our findings suggest that the immune infiltration levels were elevated in CNTRL high-expression groups. Predicted results further indicated that CNTRL expression levels influence the response to immunotherapy in gliomas. These findings offer new insights into potential immunotherapy strategies for glioma treatment.

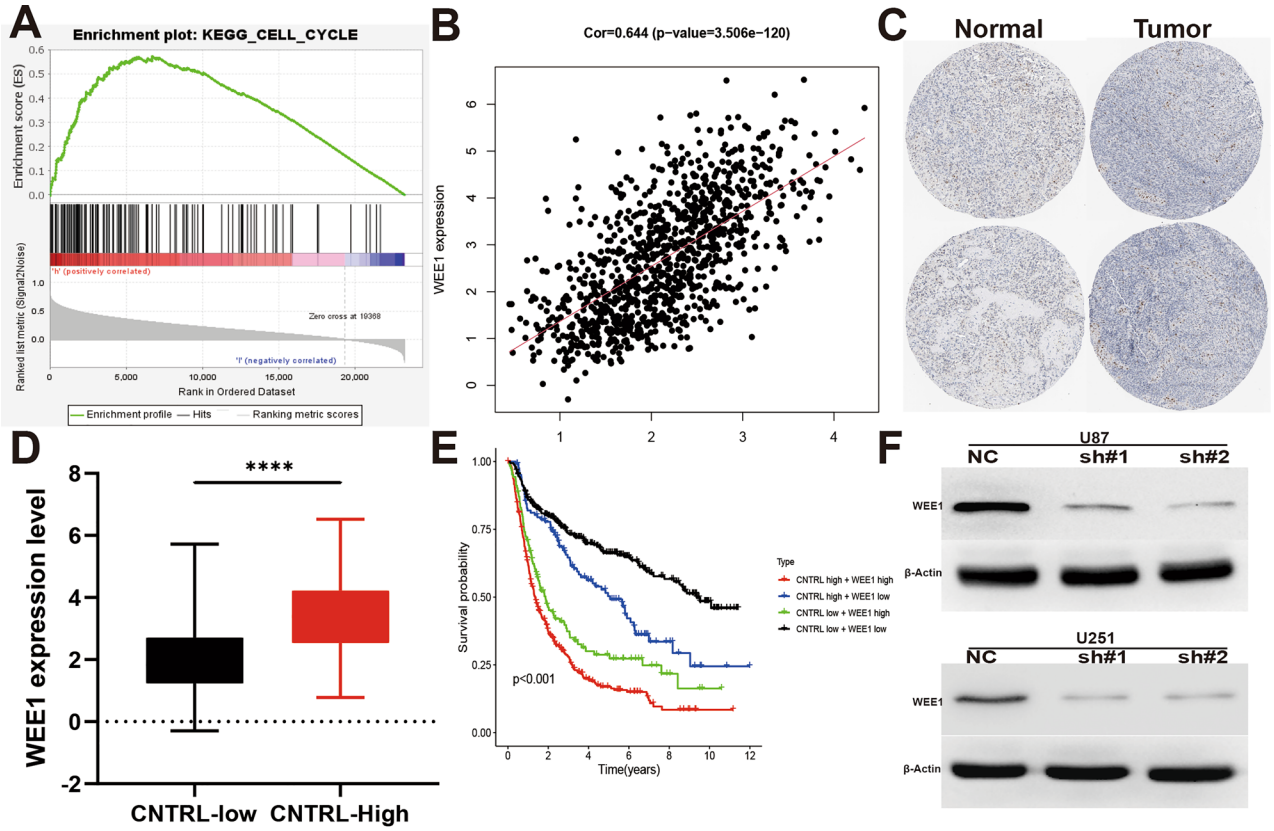
A
Enrichment plot: KEGG_CELL_CYCLE
Enrichment score (ES)
Ranked list metric (Signal2Noise)
'h' (positively correlated)
Zero cross at 19368
'l' (negatively correlated)
Rank in Ordered Dataset
Enrichment profile
Hits
Ranking metric scores
B
Cor=0.644 (p-value=3.506e-120)
WEE1 expression
C
Normal
Tumor
D
****
WEE1 expression level
CNTRL-low
CNTRL-High
E
Survival probability
p<0.001
Time(years)
Type
CNTRL high + WEE1 high
CNTRL high + WEE1 low
CNTRL low + WEE1 high
CNTRL low + WEE1 low
F
U87
NC
sh#1
sh#2
WEE1
β-Actin
U251
NC
sh#1
sh#2
WEE1
β-Actin

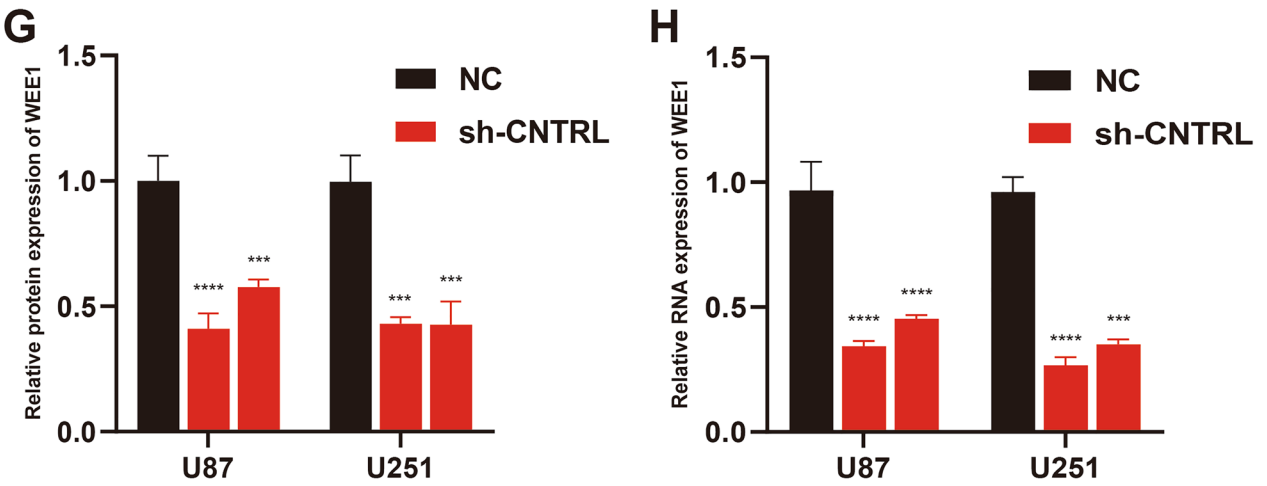
G
Relative protein expression of WEE1
NC
sh-CNTRL
U87
U251
H
Relative RNA expression of WEE1
NC
sh-CNTRL
U87
U251

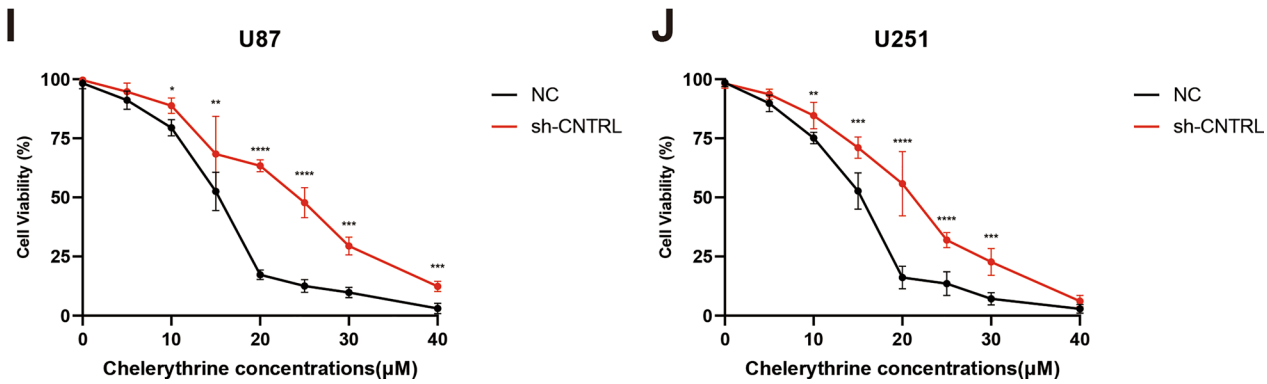
I
U87
Cell Viability (%)
Chelerythrine concentrations(μM)
NC
sh-CNTRL
J
U251
Cell Viability (%)
Chelerythrine concentrations(μM)
NC
sh-CNTRL

The primary strengths of this study include the validation of CNTRL's prognostic role in independent cohorts and the experimental confirmation of its biological functions in glioma cells. However, several limitations must be acknowledged: First, study with more large sample size is required to further verify the prognostic role of CNTRL in glioma. Second, our only validated the phenotypic function of CNTRL in glioma cells, and the specific molecular mechanism should be explored. Third, the complex mechanism between tumor microenvironment and immune infiltration needs further experimental verification and exploration. The potential effect of CNTRL on immunotherapy need to be confirmed by other datasets because the present results are from algorithm prediction. Besides, since the drug sensitivity results are derived from pan-cancer database analysis, they should be interpreted with caution and may not be directly applicable to specific patient cases. Finally, the predictive power of the nomogram risk model was 0.635 at 1 year, 0.685 at 3 years, and 0.722 at 5 years, indicating moderate diagnostic ability. The lack of high accuracy without combination with other biomarkers may limit its clinical use.

5 Conclusions

CNTRL plays a critical role in glioma progression, serving as a prognostic biomarker and a potential therapeutic target. It is overexpressed in glioma, associated with poor patient outcomes, and influences tumor biology through pathways related the cell cycle regulation, immune response, and tumor microenvironment. This study provides comprehensive insights into CNTRL's function and highlights its potential to guide future therapeutic and prognostic strategies in glioma.

Acknowledgements None.

Author Contributions Author contributions MXP drafted the manuscript. QDY and ZM collect and analyze data. QDY prepared the Figure. ZM contributed analysis tools. TH collected data. TH and ZY revised the manuscript. All authors reviewed the manuscript.

Funding This study was supported by The Guangxi Natural Science Foundation (2025GXNSFBA069308,2024GXNSFAA010252,2022GXNSFBA035576), Key Discipline of Traditional Chinese Medicine in Guangxi, "Zhuang Medicine External Therapy" (GZXK-Z-20-62), Guangxi Young and Middle-aged Teachers Ability Enhancement Project (2023KY0298), Guangxi Young Qishan Scholars Training Program(GXQH202419), 2025 Guangxi Traditional Chinese Medicine Suitable Technology Development and Promotion Project (GZSY2025086), 2024 Youth Fund Project of Guangxi University of Traditional Chinese Medicine (2024QN013), Funding for the Talent Cultivation Project of Guangxi International Zhuang Medicine Hospital's "Young Seed Project", Scientific research projects funded by Chinese medicine in 2021 (20210506), Research Project of the Chinese Ethnic Medicine Society (2022M1095-310307).

Data availability All original data can be available from the corresponding author upon request.

Declarations

Competing interests The authors declare no competing interests.

References

1. Weller M, Wick W, Aldape K, Brada M, Berger M, Pfister SM, et al. Glioma. Nat Rev Dis Primers. 2015;1:15017.
2. Chen R, Smith-Cohn M, Cohen AL, Colman H. Glioma subclassifications and their clinical significance. Neurotherapeutics. 2017;14(2):284–97.
3. Nicholson JG, Fine HA. Diffuse glioma heterogeneity and its therapeutic implications. Cancer Discov. 2021;11(3):575–90.
4. Cohen AL, Colman H. Glioma biology and molecular markers. Cancer Treat Res. 2015;163:15–30.
5. Gusyatiner O, Hegi ME. Glioma epigenetics: From subclassification to novel treatment options. Semin Cancer Biol. 2018;51:50–8.
6. Ludwig K, Kornblum HI. Molecular markers in glioma. J Neurooncol. 2017;134(3):505–12.

7. Ou YY, Mack GJ, Zhang M, Rattner JB. CEP110 and ninein are located in a specific domain of the centrosome associated with centrosome maturation. J Cell Sci. 2002;115(Pt 9):1825–35.
8. Frazer JK, Jackson DG, Gaillard JP, Lutter M, Liu YJ, Banchereau J, et al. Identification of centerin: a novel human germinal center B cell-restricted serpin. Eur J Immunol. 2000;30(10):3039–48.
9. Popovici C, Mattei MG, Rattner JB, Birnbaum D, Pebusque MJ. Assignment of the centrosomal protein 110 gene (Cep110) to mouse chromosome bands 2B–C1 by in situ hybridization. Cytogenet Cell Genet. 2000;89(3–4):216–7.
10. Montes-Moreno S, Roncador G, Maestre L, Martinez N, Sanchez-Verde L, Camacho FI, et al. Gcet1 (centerin), a highly restricted marker for a subset of germinal center-derived lymphomas. Blood. 2008;111(1):351–8.
11. Vizmanos JL, Novo FJ, Roman JP, Baxter EJ, Lahortiga I, Larrayoz MJ, et al. NIN, a gene encoding a CEP110-like centrosomal protein, is fused to PDGFRB in a patient with a t(5;14)(q33;q24) and an imatinib-responsive myeloproliferative disorder. Cancer Res. 2004;64(8):2673–6.
12. Zeng Z, Jiang X, Pan Z, Zhou R, Lin Z, Tang Y, et al. Highly expressed centromere protein L indicates adverse survival and associates with immune infiltration in hepatocellular carcinoma. Aging (Albany NY). 2021;13(19):22802–29.
13. Park TS, Song J, Kim JS, Yang WI, Song S, Kim SJ, et al. 8p11 myeloproliferative syndrome preceded by t(8;9)(p11;q33), CEP110/FGFR1 fusion transcript: morphologic, molecular, and cytogenetic characterization of myeloid neoplasms associated with eosinophilia and FGFR1 abnormality. Cancer Genet Cytogenet. 2008;181(2):93–9.
14. Ren M, Qin H, Kitamura E, Cowell JK. Dysregulated signaling pathways in the development of CNTRL-FGFR1-induced myeloid and lymphoid malignancies associated with FGFR1 in human and mouse models. Blood. 2013;122(6):1007–16.
15. Pongor L, Kormos M, Hatzis C, Pusztai L, Szabo A, Gyorffy B. A genome-wide approach to link genotype to clinical outcome by utilizing next generation sequencing and gene chip data of 6,697 breast cancer patients. Genome Med. 2015;7:104.
16. Katsurahara K, Shiozaki A, Kosuga T, Kudou M, Shoda K, Arita T, et al. ANO9 regulated cell cycle in human esophageal squamous cell carcinoma. Ann Surg Oncol. 2020;27(9):3218–30.
17. Huang C, Liu Z, Guo Y, Wang W, Yuan Z, Guan Y, et al. scCancerExplorer: a comprehensive database for interactively exploring single-cell multi-omics data of human pan-cancer. Nucleic Acids Res. 2025;53(D1):D1526–35.
18. Yuan J, Levitin HM, Frattini V, Bush EC, Boyett DM, Samanamud J, et al. Single-cell transcriptome analysis of lineage diversity in high-grade glioma. Genome Med. 2018;10(1):57.
19. Wu S, Wang S, Gao F, Li L, Zheng S, Yung W, et al. Activation of WEE1 confers resistance to PI3K inhibition in glioblastoma. Neuro Oncol. 2018;20(1):78–91.
20. Brown LM, Bartolo RC, Davidson NM, Schmidt B, Brooks I, Challis J, et al. Targeted therapy and disease monitoring in CNTRL-FGFR1-driven leukaemia. Pediatr Blood Cancer. 2019;66(10): e27897.
21. Liu F, Qu R, Yang L, Shi G, Hao S, Hu C. Circular RNA controls tumor occurrence and development via cell cycle regulation. Onco Targets Ther. 2022;15:993–1009.
22. Abreu VA, Howard MS. Tumor-suppressor genes, cell cycle regulatory checkpoints, and the skin. N Am J Med Sci. 2015;7(5):176–88.
23. Kashyap D, Garg VK, Sandberg EN, Goel N, Bishayee A. Oncogenic and tumor suppressive components of the cell cycle in breast cancer progression and prognosis. Pharmaceutics. 2021;13(4):569.
24. Xie B, Wang S, Jiang N, Li JJ. Cyclin B1/CDK1-regulated mitochondrial bioenergetics in cell cycle progression and tumor resistance. Cancer Lett. 2019;443:56–66.
25. Ouyang Q, Xu L, Cui H, Xu M, Yi L. MicroRNAs and cell cycle of malignant glioma. Int J Neurosci. 2016;126(1):1–09.
26. Candolfi M, King GD, Yagiz K, Curtin JF, Mineharu Y, Muhammad AK, et al. Plasmacytoid dendritic cells in the tumor microenvironment: immune targets for glioma therapeutics. Neoplasia. 2012;14(8):757–70.
27. Mishchenko TA, Turubanova VD, Gorshkova EN, Krysko O, Vedunova MV, Krysko DV. Glioma: bridging the tumor microenvironment, patient immune profiles and novel personalized immunotherapy. Front Immunol. 2023;14:1299064.
28. Lin C, Wang N, Xu C. Glioma-associated microglia/macrophages (GAMs) in glioblastoma: Immune function in the tumor microenvironment and implications for immunotherapy. Front Immunol. 2023;14:1123853.
29. Sun Y, Li R, Chen Y, Yang B, Li X, Li Z, et al. The value of basement membrane-associated genes in the prognosis and immune regulation of glioma. Medicine (Baltimore). 2023;102(23): e33935.
30. Cao J, Yan Q. Cancer epigenetics, tumor immunity, and immunotherapy. Trends Cancer. 2020;6(7):580–92.
31. Xu S, Tang L, Li X, Fan F, Liu Z. Immunotherapy for glioma: Current management and future application. Cancer Lett. 2020;476:1–12.
32. Gallus M, Kwok D, Lakshmanachetty S, Yamamichi A, Okada H. Immunotherapy approaches in isocitrate-dehydrogenase-mutant low-grade glioma. Cancers (Basel). 2023;15(14):3726.
33. Huang Q, Pan X, Zhu W, Zhao W, Xu H, Hu K. Natural products for the immunotherapy of glioma. Nutrients. 2023;15(12):2795.
34. Bunse L, Bunse T, Kramer C, Chih YC, Platten M. Clinical and translational advances in glioma immunotherapy. Neurotherapeutics. 2022;19(6):1799–817.